Supplemental Figure 1 -- related to Figure 1

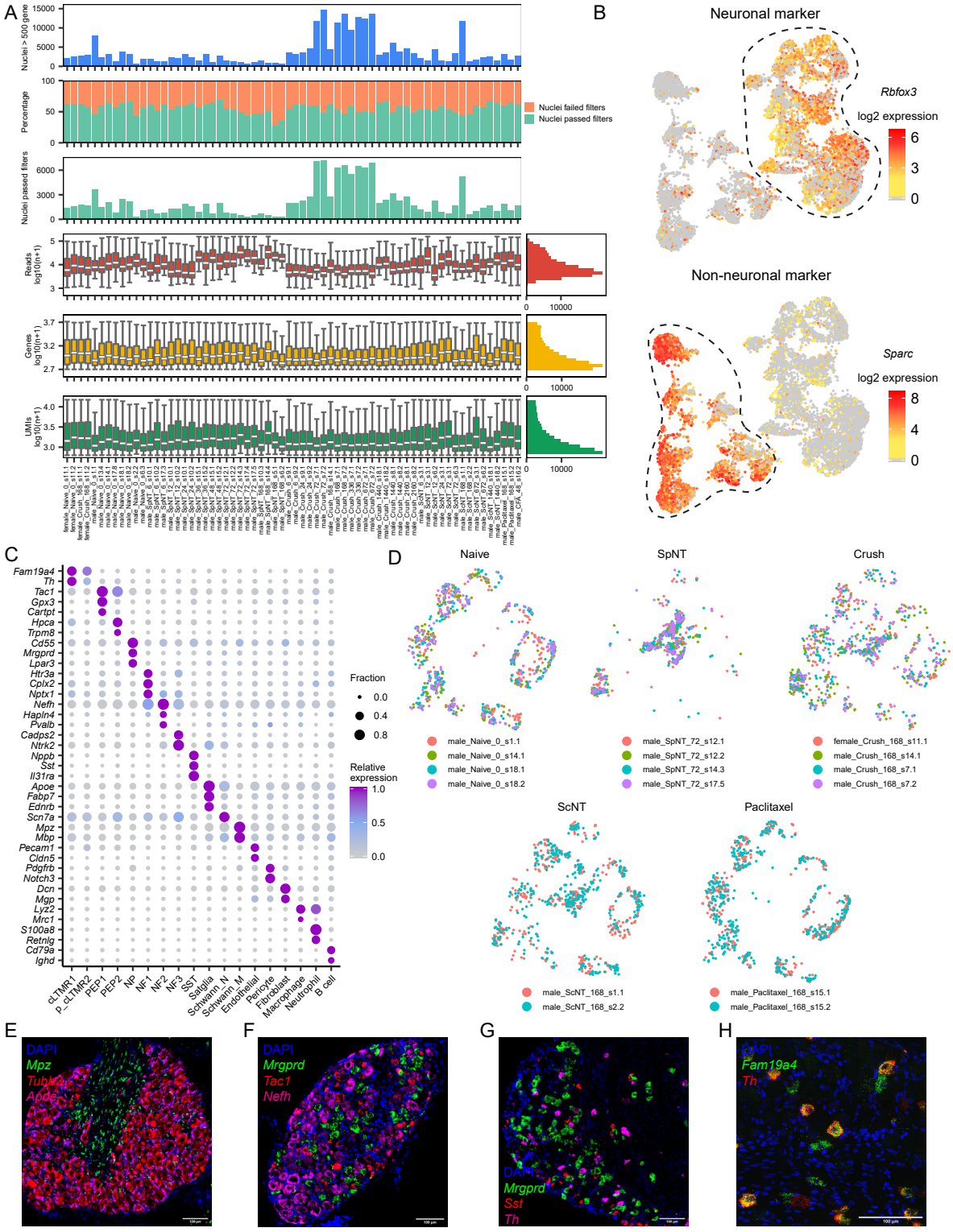

Figure S1, related to Figure 1. Single-nucleus RNA-seq of mouse DRG before and after peripheral nerve injury.

(A) Sequencing metrics for each library included in the study. Number of nuclei per sample with > 500 unique genes (top box) and the fraction of these nuclei that passed quality control filters (second box). Number of nuclei that passed quality control for each sample and used for downstream analysis (third row). Box plots display number of total reads per nucleus (log_{10} transformed, fourth row), genes per nucleus (log_{10} transformed, fifth row), and unique molecular identifiers (UMI) per nucleus (log_{10} transformed, bottom row). Boxes indicate quartiles and whiskers are 1.5-times the interquartile range (Q1-Q3). The median is a white line inside each box. The distribution is aggregated across all samples and displayed on the horizontal histogram.
(B) UMAP plots of 10,000 randomly sampled nuclei from the 141,093 nuclei passing quality control in the study. Nuclei are colored by their log_2 expression of the neuronal marker gene *Rbfox3* (top) and non-neuronal marker gene, *Sparc* (bottom).
(C) Dot plot of cell-type-specific marker genes (rows) in each naive DRG cell type (columns). The fraction of nuclei expressing a marker gene is calculated as the number of nuclei in each cell type that express a gene (>0 counts) divided by the total number of naive nuclei in the respective cell type. Expression in each cell type is calculated as mean expression of a gene relative to the highest mean expression of that gene across all cell types.
(D) UMAP plots of 800 randomly sampled nuclei from 2-4 biological replicates of the experimental conditions displayed. Nuclei are colored by their biological replicate. Each cluster has a mix of nuclei from each replicate, suggesting there are minimal if any batch effects between replicates.
(E-G) FISH images of naive L4 mouse DRGs stained with DAPI (blue), *Mpz* (myelinating Schwann cell marker, green), *Tubb3* (neuronal marker, red) and *Apoe* (satellite glia marker, magenta) (E); *Mrgprd* (NP [non-peptidergic] DRG neuronal marker, green), *Tac1* (PEP [peptidergic] DRG neuronal marker, red) and *Nefh* (NF [neurofilament+] DRG neuron marker, magenta) (F); *Mrgprd* (NP DRG neuron marker, green), *Sst* (*Sst*+ pruriceptive DRG neuron marker, red) and *Th* (cLTMR DRG neuron marker, magenta) (G). There is minimal overlap between marker gene fluorescence, suggesting these genes are expressed in distinct cell types. Scale bar = 100μm.
(H) Representative FISH images of naive L4 mouse DRGs stained with DAPI (blue), *Fam19a4* (cLTMR1 and p_cLTMR2 marker, green) and *Th* (c-LTMR1 marker, red). Some cells express both *Th* and *Fam19a4* at high levels (cLTMR1), while others express *Fam19a4* with little to no *Th* expression (p_cLTMR2). Scale bars = 100μm.
cLTMR = C-fiber low threshold mechanoreceptor; PEP = peptidergic nociceptor; NP = non-peptidergic nociceptor; NF = *Nefh*+ A-fiber low threshold mechanoreceptors; SST = *Sst*+ pruriceptors; Satglia = satellite glia, Schwann_M = myelinating Schwann cells, Schwann_N = nonmyelinating Schwann cells.

Supplemental Figure 2 -- related to Figure 1

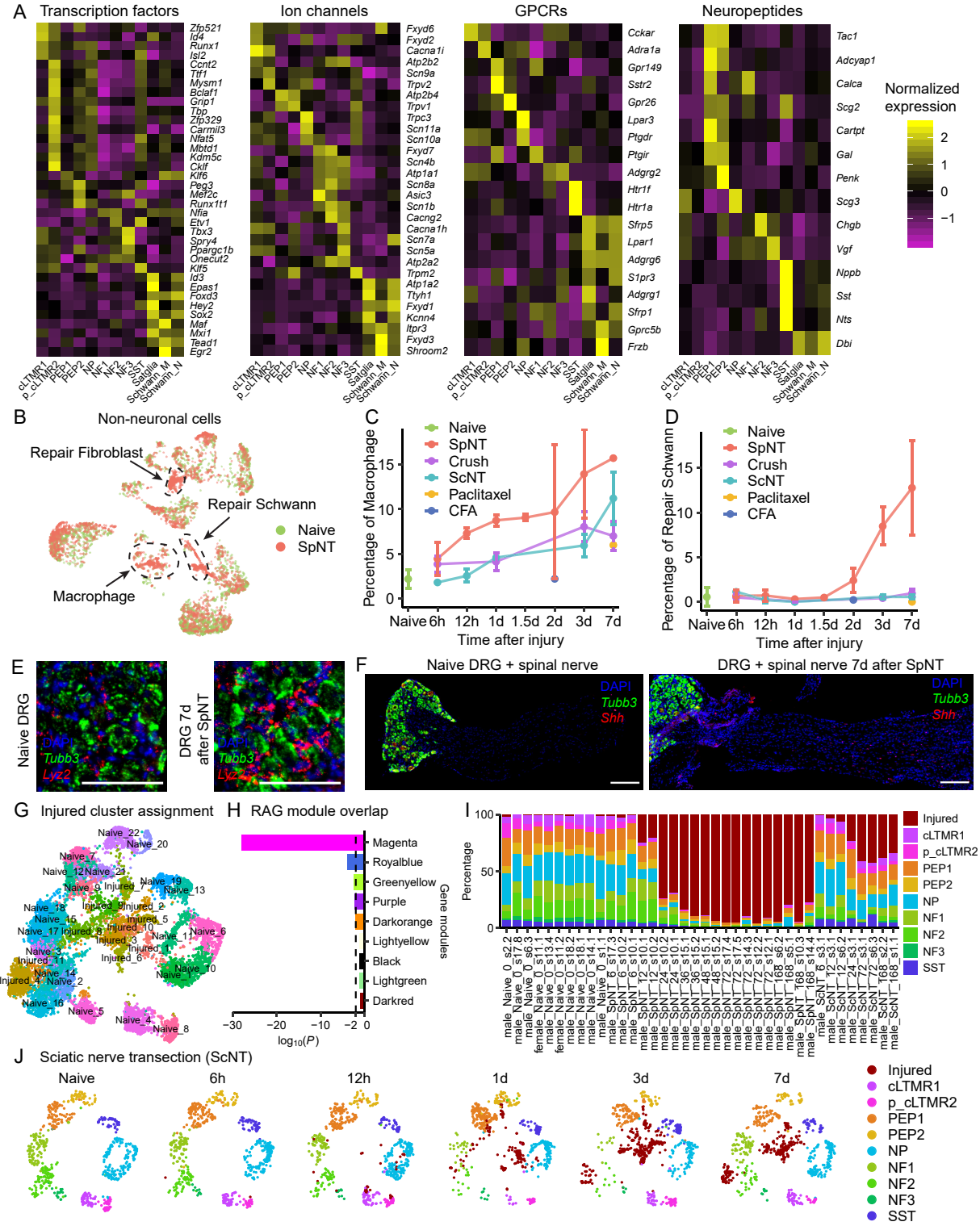

Figure S2, related to Figure 1. Characterization of DRG neuronal gene expression before and after peripheral nerve injury.

(A) Heatmaps of cell-type-specific gene expression patterns in naive DRG cell types. Genes are included in the heatmap if they are significantly enriched in a cell type compared to all other cell types (FDR < 0.01, $\log_2$FC > 1, using FindMarkers in Seurat, see Table S2) and matched the displayed gene ontology annotations (see methods). Heatmaps show row-normalized and centered mean expression of each gene in a given cell type.
(B) UMAP plot of 2,000 non-neuronal DRG nuclei from naive mice (green) and 2,000 non-neuronal DRG nuclei from spinal nerve transection mice (SpNT, red). The vast majority of naive and SpNT nuclei cluster together, but two small SpNT-specific clusters emerge (see arrows).
(C) Percentage of macrophages out of all non-neuronal DRG cells in each injury model displayed. There is an increase in the fraction of macrophages in the DRG after SpNT and 7d of paclitaxel treatment but not 2d after CFA injection.
(D) Percentage of *Shh*+ repair Schwann cells out of all non-neuronal cells in each injury model displayed. There is an increase in the fraction of repair Schwann cells over time in the SpNT samples but not after 7d of paclitaxel treatment or 2d after CFA injection. It is important to note that most if not all of the repair Schwann cells observed in the SpNT snRNAseq samples likely reside in the axotomized proximal nerve stump rather than in the DRG itself. This is because cells from the proximal nerve stump can be sequenced together with the DRG given the proximity of the DRG to the injury site.
(E) FISH of L4 DRGs from naive mice (left) or 7d after SpNT (right), stained with DAPI (blue), *Tubb3* (green) and *Lyz2* (red). There is an increase in *Lyz2* fluorescence after SpNT, suggesting an infiltration of *Lyz2*+ immune cells into the DRG. Scale bar = 100μm.
(F) FISH of L4 DRG and spinal nerve from naive mice (left) or 7d after SpNT (right), stained with DAPI (blue), *Tubb3* (green) and *Shh* (red). There is an increase in the number of *Shh*+ cells in the spinal nerve after SpNT. Scale bar = 200μm.
(G) UMAP plot of 10,000 randomly sampled neurons that passed quality control from naive mice and mice from each injury model. Clusters are colored by the K-nearest neighbors cluster ID assigned by Seurat. The names of each cluster reported in Figure 1E are overlaid on their respective cluster.
(H) Overlap between injury-induced genes from the single-nucleus RNA-seq study (FDR < 0.01 and $\log_2$FC > |1|, injured state nuclei after SpNT vs. nuclei from naive animals) and injury-related gene modules previously identified (Chandran et al., 2016). The $\log_{10}$ transformed hypergeometric *P*-values from each pair-wise comparison of the injury-induced genes in our study and those in a module from Chandran et al., are displayed. The vertical dashed line is at $P = 0.01$. In Chandran et al., modules were identified by co-expression network analysis of gene expression differences between bulk DRG tissue from naive mice and mice subjected to several peripheral nerve injury models. The magenta module is the predominant injury-induced gene module in Chandran et al. and has the greatest overlap with the “injured” transcriptional state in our study.
(I) Percentage of neuronal nuclei from each biological sample (naive, spinal nerve transection [SpNT], sciatic nerve transection+ligation [ScNT]) classified into respective DRG cell types. Neurons classified as in injured state are shown in red.
(J) UMAP plots displaying naive DRG neurons and DRG neurons after sciatic nerve transection. Each time point displays 650 neuronal nuclei randomly sampled to display the same number of nuclei over time. Nuclei are colored by their cell type.

cLTMR = C-fiber low threshold mechanoreceptor; PEP = peptidergic nociceptor; NP = non-peptidergic nociceptor; NF = *Nefh*+ A-fiber low threshold mechanoreceptors; SST = *Sst*+ pruriceptors.

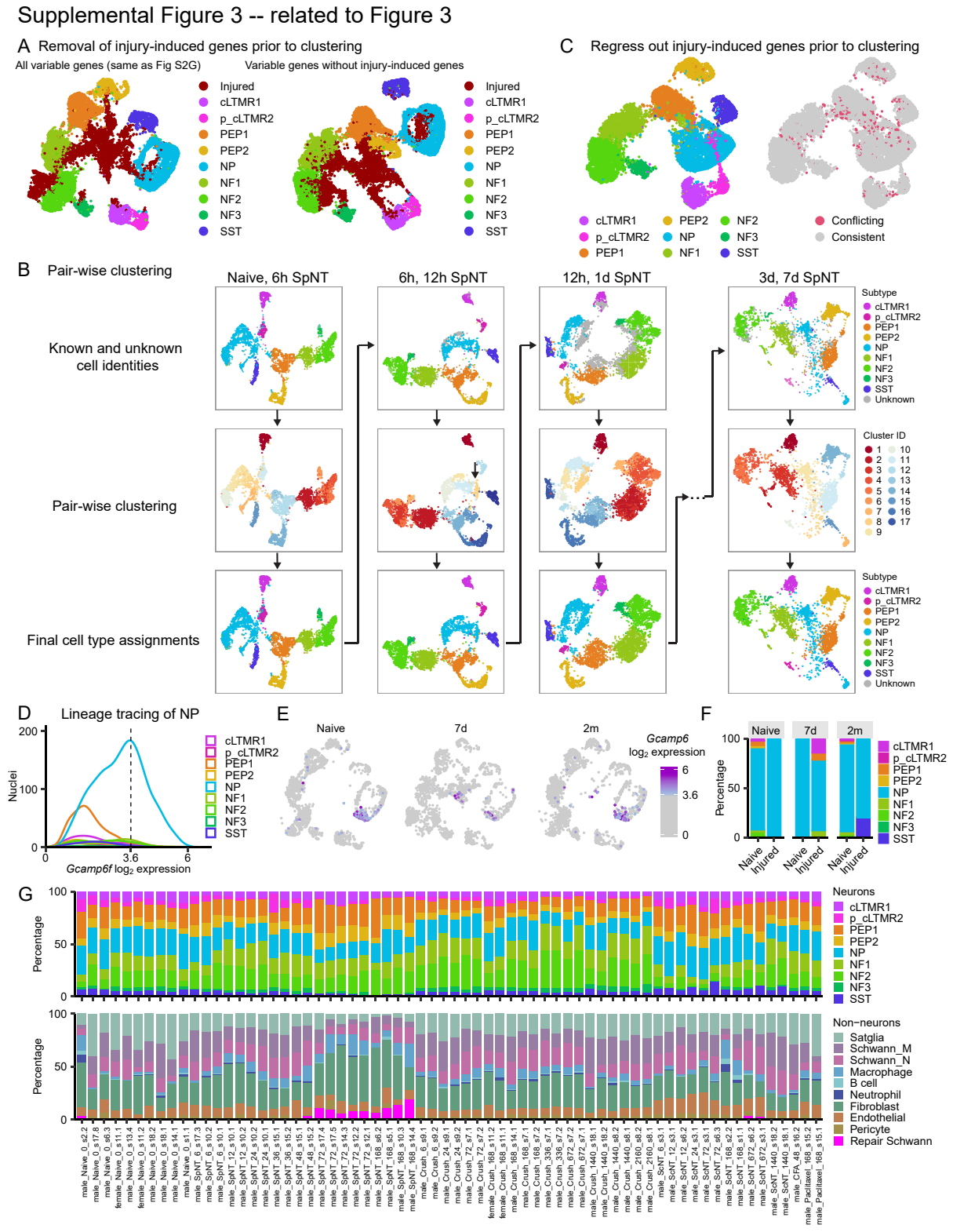

Figure S3, related to Figure 3. Classification of injured DRG neuronal subtypes after spinal nerve transection (SpNT).

(A) UMAP plots showing 7,000 naive neuronal nuclei and 7,000 randomly sampled neuronal nuclei from all time points after SpNT using all variable genes identified for clustering (left, see methods) or the variable genes remaining after removing injury-induced genes (FDR < 0.01, $log_2FC > 1$, injured state nuclei after SpNT vs. nuclei from naive animals) (right) for clustering. Colors denote cell types.
(B) Pairwise clustering and projection strategy to classify the neuronal subtypes of injured state nuclei after SpNT. Nuclei of known and unknown neuronal subtypes from each SpNT time point are co-clustered with the subsequent time point collected (top row). Nuclei of unknown neuronal subtype that co-cluster with clusters of marker-gene-confirmed known neuronal subtypes (middle row), were then assigned the respective neuronal subtype of that cluster (bottom row, see methods). The new injured neuronal subtype assignments were projected forward to assist in the subtype assignment of injured neurons at later time points after SpNT (long arrows). Each column shows co-clustering of nuclei from two adjacent time points. Top row colors indicate neuronal subtype with unknown injured nuclei colored gray. Middle row colors indicate cluster IDs assigned by Seurat. Bottom row colors indicate the final subtype assignment after pair-wise clustering and projection. Pair-wise clustering and projection for time points between 1d and 3d after SpNT are not shown for simplicity.
(C) UMAP plot showing 7,000 randomly sampled naive neuronal nuclei and 7,000 randomly sampled SpNT neuronal nuclei. Clustering was performed after regressing out the injury-induced genes (FDR < 0.01, $log_2FC > 1$, injured state nuclei after SpNT vs. nuclei from naive animals) from the mRNA counts tables (see methods). Colors denote the neuronal subtype assignment using regression-based clustering (left) or the concordance between neuronal subtype assignments using the two independent approaches: pairwise clustering and projection and regression-based clustering (right).
(D) Cell-type tracing of non-peptidergic nociceptors (NPs) to experimentally test neuronal subtype bioinformatic assignments. A histogram of all *Mrgprd-Cre^{ERT2}*;*Gcamp6f* neuronal nuclei in the study with *Gcamp6f* expression > 0 as a function of *Gcamp6f* log_2 expression. The threshold *Gcam6f* log_2 expression (3.6) for a nucleus to be considered “reporter-positive” is indicated by the dotted line.
(E) UMAP plots of DRG neurons from *Mrgprd-Cre^{ERT2}*;*Gcamp6f* reporter mice. 1,913 neurons are displayed from naive mice (left), 1,913 neurons are displayed 7d after Crush (middle), and 1,913 neurons are displayed 2mo after Crush (right). Nuclei are colored by *Gcamp6f* log_2 expression (nuclei with *Gcamp6f* log_2 expression ≤ 3.6 are colored gray).
(F) The neuronal subtypes assigned to reporter-positive *Mrgprd-Cre^{ERT2}*;*Gcamp6f* neuronal nuclei. The percentages of each neuronal subtype assigned to reporter-positive neuronal nuclei are shown, with 71-100% of reporter-positive neuronal nuclei classified as NP. Colors indicate cell type. d = days, m = months.
(E) Fraction of cell types within individual biological samples sequenced after classification of neuronal subtypes in the injured state. The top graph displays neuronal subtypes and the bottom graph displays non-neuronal cell types. The number above of each bar shows total number of nuclei for each sample that passed quality control.
cLTMR = C-fiber low threshold mechanoreceptor; PEP = peptidergic nociceptor; NP = non-peptidergic nociceptor; NF = *Nefh*+ A-fiber low threshold mechanoreceptors; SST = *Sst*+ pruriceptors; Satglia = satellite glia, Schwann_M = myelinating Schwann cells, Schwann_N = nonmyelinating Schwann cells.

Supplemental Figure 4 -- related to Figure 4

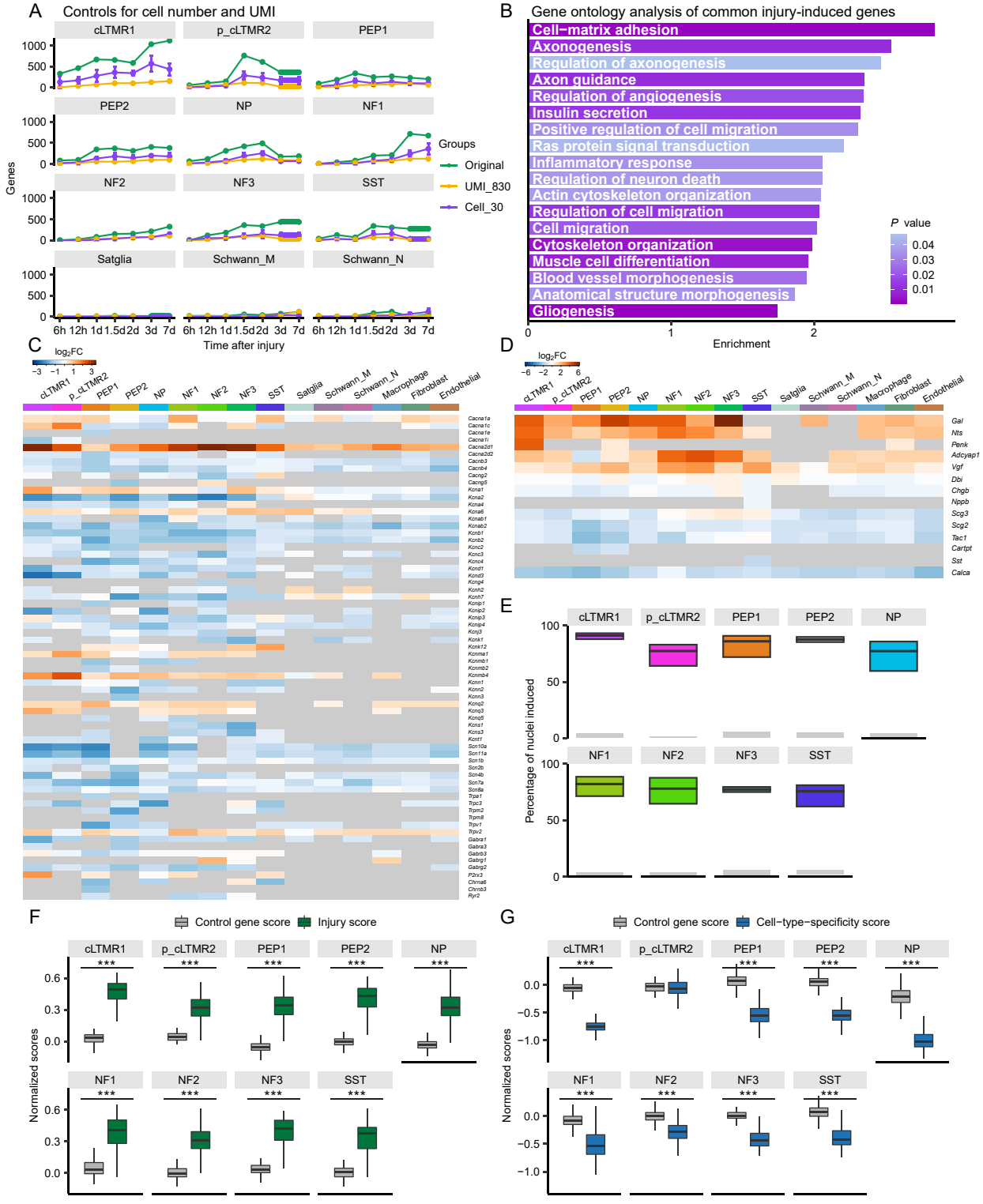

Figure S4, related to Figure 4. Cell-type specific transcriptional changes in DRG neurons after spinal nerve transection (SpNT).

(A) Control analysis to test influence of cell number and UMI on differential gene expression. Number of significantly induced genes (FDR < 0.01, $log_2FC > 1$) in each cell type and time point after SpNT compared to naive nuclei of the respective subtype. The number of genes induced by injury increases over time regardless of UMI or number of nuclei, although the absolute number of statistically significant genes decreases if fewer nuclei or UMI/nucleus are used for differential expression analysis. Lines: original = differential expression including all nuclei that pass quality control in a given cell type and time point (green). UMI_830 = prior to differential expression, nuclei from all time points and cell type are down-sampled to an average of 830 UMI (the lowest average UMI in the SpNT time course, see methods). Cell_30 = downsampling of each cell type to 30 nuclei prior to differential expression. Differential expression analysis was performed on 10 independent down-samplings of 30 nuclei for each cell type and time point and mean number of genes across these 10 analyses is displayed. Error bars represent standard deviation in the number of differentially regulated genes across the 10 analyses. The thick horizontal bar between the 3 and 7d SpNT time points in p_cLTMR2, NF3, SST, and Satglia indicate that cells from these time points were combined to increase power.
(B) Gene ontology analysis (topGO) of the 524 genes commonly induced in ≥ 5 neuronal subtypes after SpNT compared to naive neurons (see Table S4). The gene ontology terms displayed in the graph are terms that have > 14 annotated significant genes and *P*-value < 0.05. Enrichment is the number of times an ontology term is observed in the common injury gene set over a random gene set of expressed genes. Bars are colored by *P*-value.
(C) Heatmap of the log_2FC (3d and 7d SpNT nuclei compared to naive nuclei for each cell type) of select genes encoding ion channels. Genes shown on the heatmap are significantly regulated (FDR < 0.01, $log_2FC > |1|$) in at least one cell type after SpNT.
(D) Heatmap of the log_2FC (3d and 7d SpNT nuclei compared to naive nuclei for each cell type) of select genes encoding neuropeptides. Genes shown on the heatmap are significantly regulated (FDR < 0.01, $log_2FC > |1|$) in at least one cell type after SpNT.
(E) Estimate of the fraction of nuclei that induce the common injury gene program after SpNT. A nucleus was classified as "induced" by injury if it expressed a threshold number of injury-response genes: the upper bar of the box is defined by the fraction of SpNT nuclei expressing 3 injury genes/nucleus, the central line is the fraction of SpNT nuclei expressing 4 injury genes/nucleus, and the lower bar is the fraction of SpNT nuclei expressing 5 injury genes/nucleus. Grey rectangles show the fraction of nuclei from naive animals that express 3 injury genes/nucleus (upper boundary) or 5 injury gene/nucleus (lower boundary). The set of injury-induced genes used to classify nuclei as "induced" was chosen from the 10 common injury genes from Figure 4C/Table S4 with greatest fold-change between SpNT 3d after injury and naive (*Atf3, Cdkn1a, Flrt3, Gadd45a, Gadd45g, Itga7, Jun, Sema6a, Sox11, Tifa*). A gene is considered "expressed" in a nucleus if its log_2 expression is > 90^{th} percentile of all naive nuclei of the same cell type.
(F) Box plots showing the injury score (green) and a control score generated from a set of expression-matched genes (gray, see methods) in each cell type 3-7d after SpNT. Scores are normalized to the naive average. Boxes indicate quartiles of expression, and whiskers are 1.5-times the interquartile range (Q1-Q3). The median is a black line inside each box. ****P* < 0.001 two-tailed Student's t-test.

(G) Box plots showing the cell-type-specificity score (blue) and a control score generated from a set of expression-matched genes (gray, see methods) in each cell type 3 and 7d after SpNT. Scores are normalized to the naive average. Boxes indicate quartiles of expression, and whiskers are 1.5-times the interquartile range (Q1-Q3). The median is a black line inside each box. ***$P < 0.001$ two-tailed Student's t-test.
cLTMR = C-fiber low threshold mechanoreceptor; PEP = peptidergic nociceptor; NP = non-peptidergic nociceptor; NF = *Nefh*+ A-fiber low threshold mechanoreceptors; SST = *Sst*+ pruriceptors; Satglia = satellite glia, Schwann_M = myelinating Schwann cells, Schwann_N = nonmyelinating Schwann cells.

Supplemental Figure 5 -- related to Figure 5

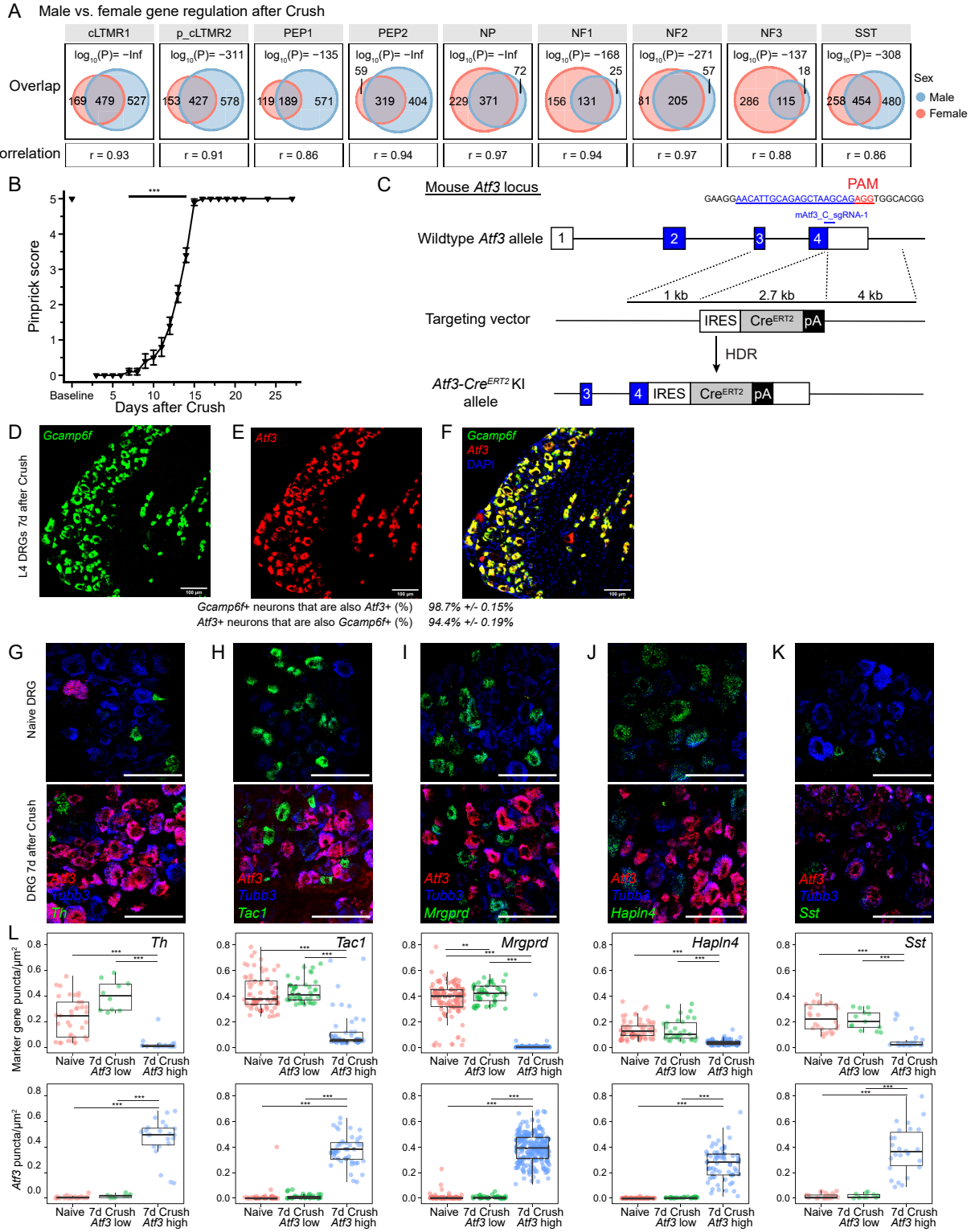

Figure S5, related to Figure 5. Molecular characterization of DRG neurons after sciatic nerve crush.

(A) Sex differences in gene expression after sciatic nerve crush. Venn diagrams display the overlap between the genes which are significantly regulated by sciatic crush compared to naive (FDR < 0.01, log_2FC > |1|, injured state neurons 1w after Crush vs. neurons from naive mice) in male and female mice. Hypergeometric test *P*-values are displayed for the overlap between male and female injury-driven gene expression changes. Pearson correlations of male and female injury-driven gene expression changes (Log_2FC, Crush vs. naive) for the set of genes significantly regulated by Crush in male or female (FDR < 0.01, log_2FC > |1|, injured state neurons 1w after Crush vs. naive) for each cell type.
(B) Recovery of sensory function after sciatic nerve crush as measured by the pinprick assay in female C57BL/6J mice. Pinprick responses recover to baseline 15d after sciatic crush (n=11 female mice, 1-way repeated measured ANOVA, $F(1, 10) = 1180$, $P = 1x10^{-11}$, Bonferroni post-hoc, ***$P < 0.001$).
(C) Diagram of the *Atf3* locus in *Atf3-Cre^{ERT2}* transgenic mice. An IRES_*Cre^{ERT2}*_pA cassette was inserted using CRISPR at the 3'UTR of the mouse *Atf3* locus to minimize interference with endogenous *Atf3* expression.
(D-F) FISH of an *Atf3-Cre^{ERT2}*;G*camp6f* L4 DRG 1w after sciatic nerve crush stained with probes against *Gcamp6f* (green, D), *Atf3* (red, E), and colocalization of DAPI (blue), *Gcamp6f* (green) and *Atf3* (red) (F). There is a very high degree of colocalization of *Atf3* and the *Gcamp6f* reporter, which is quantified below the figure and suggests that the mouse is a reliable injury reporter. Scale bar = 100μm.
(G-K) FISH images of L4 DRGs from naive mice (top) and mice 1w after sciatic crush (bottom) stained with probes against *Atf3* (H-L, red), *Tubb3* (H-L, blue) and *Th* (H, green), *Tac1* (I, green), *Mrgprd* (J, green), *Hapln4* (K, green) or *Sst* (L, green). Scale bar = 100μm.
(L) Quantification of FISH puncta from Figures S4H-L. DRG neurons were first identified by *Tubb3* fluorescence, then divided into *Atf3*-high (injured) and *Atf3*-low (naive) populations (see methods). Dots in the box plots represent mRNA quantification for individual cells, boxes indicate quartiles of expression, and whiskers are 1.5-times the interquartile range (Q1-Q3). The median is a black line inside each box. Significance testing by 1-way ANOVAs were all $P < 0.001$: Th (n = 36 [naive], 10 [7d *Atf3* low], 23 [7d *Atf3* high]), $F(2, 66) = 38.34$, *Atf3* (on Th slides), $F(2, 66) = 209.09$; Tac1 (n = 68 [naive], 40 [7d *Atf3* low], 45 [7d *Atf3* high]), $F(2, 150) = 85.03$, *Atf3* (on Tac1 slides), $F(2, 150) = 420.46$; Mrgprd (n = 100 [naive], 41 [7d *Atf3* low] , 209 [7d *Atf3* high]), $F(2, 347) = 899.72$, *Atf3* (on Mrgprd slides), $F(2, 347) = 780.13$; Hapln4 (n = 80 [naive], 32 [7d *Atf3* low] , 62 [7d *Atf3* high]), $F(2, 171) = 57.81$, *Atf3* (on Hapln4 slides), $F(2, 171) = 235.85$; Sst (n = 26 [naive], 13 [7d *Atf3* low], 26 [7d *Atf3* high]), $F(2, 62) = 29.31$, *Atf3* (on Sst slides), $F(2, 62) = 74.81$; Tukey HSD post-hoc testing (***: $p < 0.001$, **: $p < 0.01$, *: $p < 0.05$). Neurons expressing each marker gene are abundant in *Atf3*-low DRG neurons 1w after sciatic crush, whereas *Atf3*-high DRG neurons contain significantly fewer marker gene puncta.
cLTMR = C-fiber low threshold mechanoreceptor; PEP = peptidergic nociceptor; NP = non-peptidergic nociceptor; NF = *Nefh*+ A-fiber low threshold mechanoreceptors; SST = *Sst*+ pruriceptors.

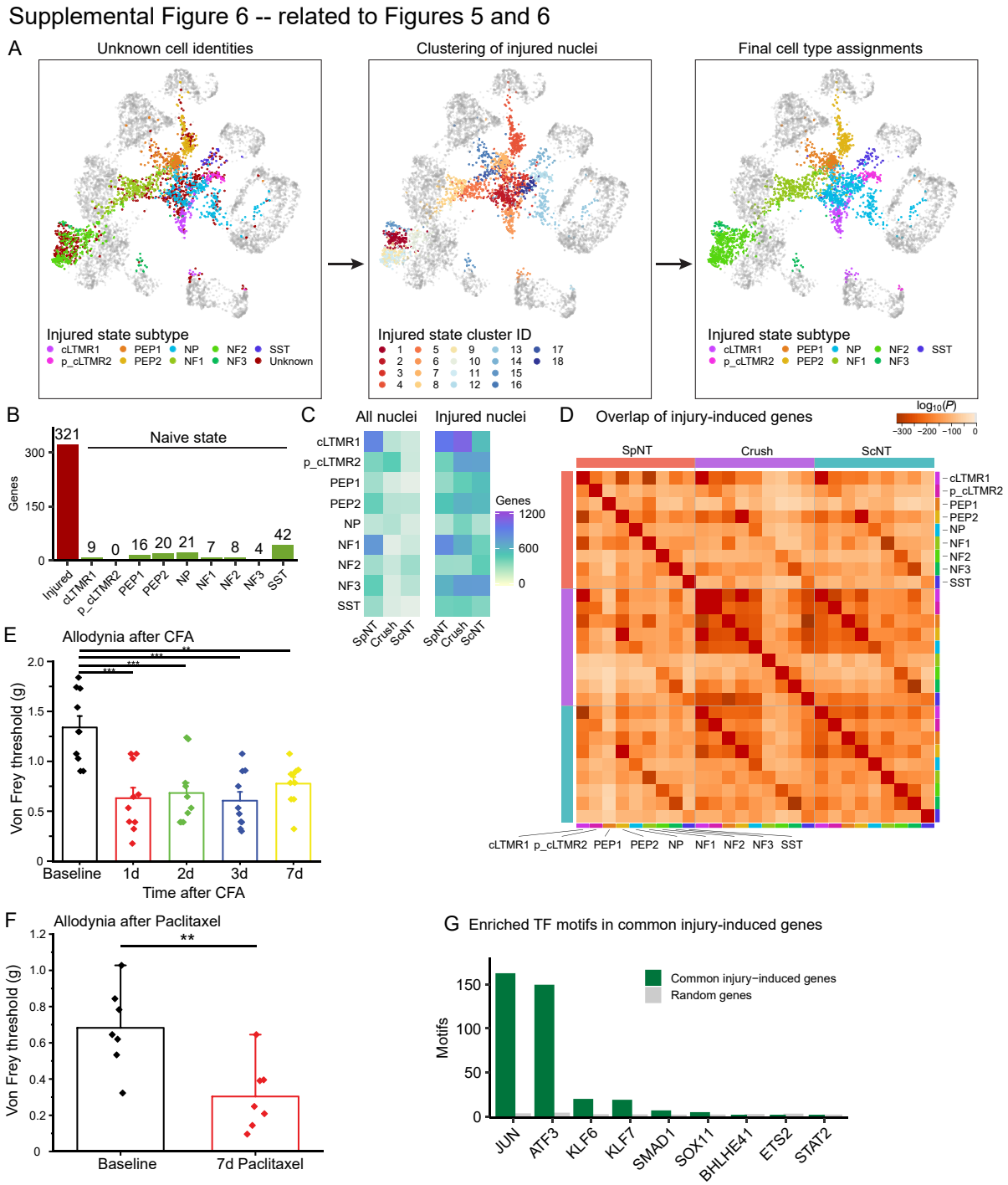

Figure S6, related to Figure 5. Comparison of transcriptional changes induced by peripheral nerve injury and other animal models of pain in DRG neurons.

(A) Co-clustering of injured state neuronal subtypes after spinal nerve transection (SpNT) with injured state neuronal subtypes after sciatic crush and sciatic nerve transection and ligation (ScNT). UMAP plots display 2,000 neurons randomly sampled from naive mice, and 2,000 neurons randomly sampled from mice subjected to each of the three injury models after they were clustered together. The neuronal subtypes of injured neurons after SpNT were previously determined by pair-wise clustering and projection. Injured nuclei from crush and ScNT of unknown neuronal subtype (left) which co-cluster with known neuronal subtypes from SpNT (middle, nuclei colored by clusterID), were then assigned the corresponding neuronal subtype (right, see methods). Nuclei are colored by their neuronal subtype (left, right) with naive state neurons colored gray.
(B) Bar plot showing the number of significantly upregulated genes (FDR < 0.01, $\log_2$FC > 1, sciatic crush mice at 7d vs. naive mice) in both injured and naive state DRG neurons after sciatic crush injury (~50% of DRG L3-5 DRG neurons are axotomized in this model). Gene expression in naive state neurons after sciatic crush (e.g. naive state nuclei from injured animals) is compared to naive neurons of the corresponding subtype. Gene expression in injured neurons after crush (e.g. injured state nuclei from injured animals) is compared to all naive neurons. Red bar corresponds to injured transcriptional state, green bars correspond to naive transcriptional state.
(C) Heatmap of the number of significantly upregulated genes in each cell type when comparing nuclei from each injury model to naive nuclei. Differential expression analyses were performed either by comparing all nuclei 3d and 7d after SpNT, crush, or ScNT vs. nuclei from the respective neuronal subtype in naive animals (left) or by comparing only nuclei in the injured state 3d and 7d after injury to the respective neuronal subtype from naive mice (right). The advantage of performing differential expression on all nuclei (left) is that we can identify cell-type-specific gene expression changes at early time points after injury prior to the emergence of the injured state, although these analyses are limited by the inclusion of unaxotomized neurons in the analysis. Performing differential expression specifically on injured nuclei allows us to more directly compare gene expression programs between injury models without including unaxotomized neurons. Because the SpNT model axotomizes most neurons, while crush and ScNT only axotomize ~50% of neurons, the similar number of gene expression changes between injured state neurons across the three models suggest the gene expression program at the level of an individual injured neuron is quite similar between distal and proximal axonal injury. The number of nuclei used for differential expression analysis in each neuronal subtype was equal across injury models and down-sampled to the number of nuclei in the injury model with the fewest number of nuclei.
(D). Pair-wise comparison of the overlap between significantly upregulated genes in injured state neuronal subtypes 3-7d after SpNT, sciatic crush, or ScNT compared to naive nuclei of the respective cell type (FDR < 0.01, $\log_2$FC > 1). This figure is distinct from Figure 5H because only neurons in the injured state are used for differential expression analysis for the reasons outlined in Figure 6B legend. Each square is colored by the *P*-value for the overlap between each comparison (hypergeometric test). Note that comparisons between the same gene list will always have 100% overlap but will have different hypergeometric *P*-values depending on list size.
(D) Von Frey behavioral measurement of mechanical sensitivity in C57BL/6J mice after hindpaw injection of 20µL CFA. CFA treatment causes significant mechanical allodynia

24h after treatment that persists for at least 7d after treatment (n=10 mice, 1-way repeated measured ANOVA, $F(4, 36) = 12.3$, $P = 0.005$, Bonferroni post-hoc $^{**}P < 0.01$, $^{***}P < 0.001$).
(F) Von Frey behavioral measurement of mechanical sensitivity in C57BL/6J mice at baseline or 1w after every-other-day treatment with 4mg/kg paclitaxel. Paclitaxel treatment causes a significant mechanical allodynia 1w after start of treatment (n = 7 mice, paired two-tailed Student's t-test, $^{**}P = 0.006$).
(G) Bar graph showing the number of early injury-induced transcription factor binding motifs present in the 524 genes commonly upregulated after injury across cell types (see Table S4). As a control, we identified the number of transcription factor binding motifs enriched in 524 randomly-selected expressed genes, and repeated this analysis 1000 times. Gray bars show the average number of transcription factor binding motifs enriched in these 1000 sets of 524 randomly-selected expressed genes.
cLTMR = C-fiber low threshold mechanoreceptor; PEP = peptidergic nociceptor; NP = non-peptidergic nociceptor; NF = *Nefh*+ A-fiber low threshold mechanoreceptors; SST = *Sst*+ pruriceptors.

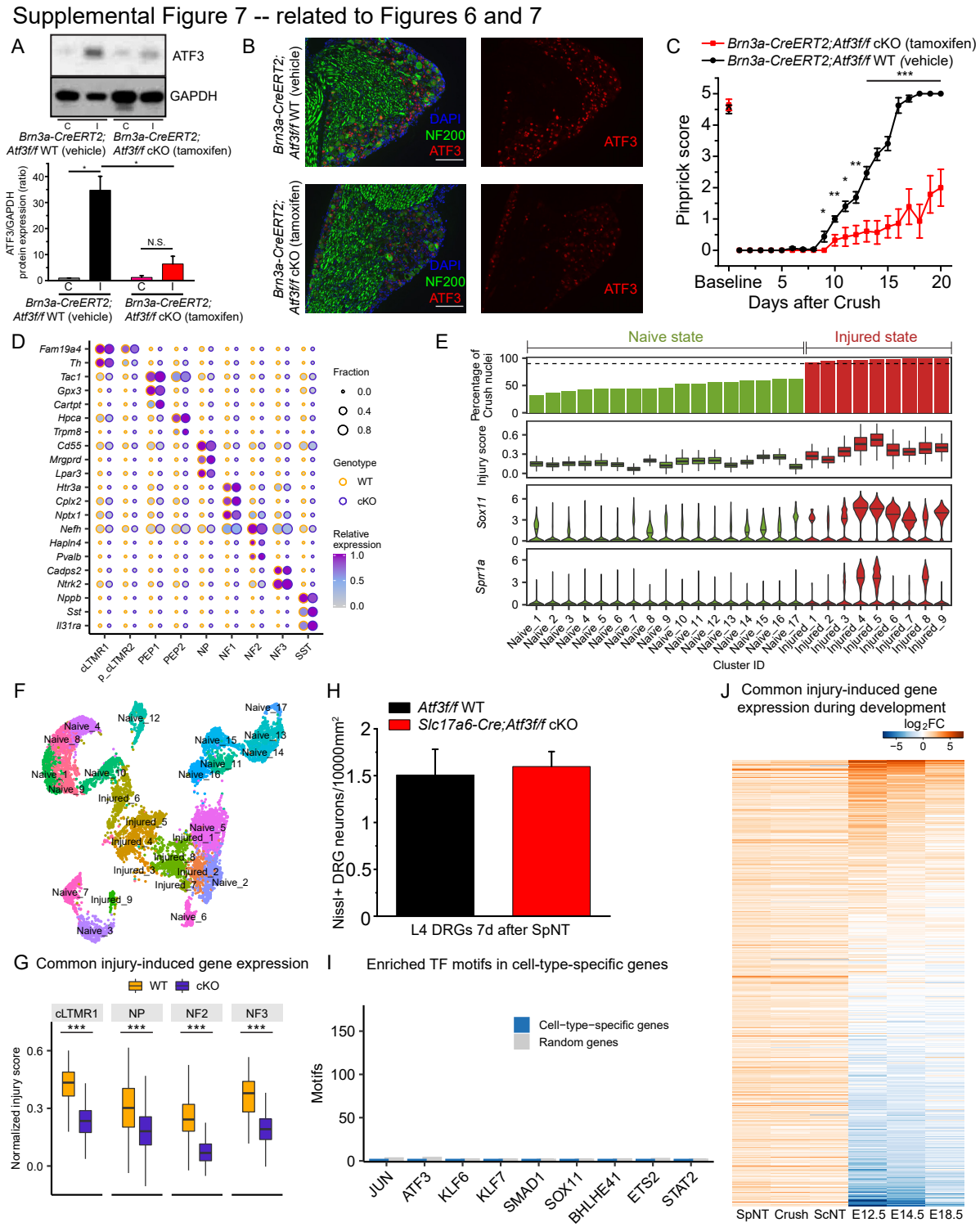

Figure S7, related to Figure 7. Transcription factor analysis of the injury-induced gene expression program.

(A) Representative Western Blot (top) and its quantification (bottom) of ATF3 protein in DRG protein extracted from ipsilateral and contralateral L3-L5 DRG neurons from *Brn3a-Cre^{ERT2};Atf3f/f* mice 1w after sciatic nerve crush. ATF3 is significantly induced in ipsilateral injured but not in uninjured contralateral DRG neurons in *Brn3a-Cre^{ERT2};Atf3f/f* mice treated with vehicle (WT control) ($p=0.04$, n=2, two-tailed Student's t-test). In *Brn3a-Cre^{ERT2};Atf3f/f* mice treated with tamoxifen (Atf3 cKO), Atf3 is not significantly induced in ipsilateral L3-L5 DRG neurons 1w after sciatic nerve crush ($p=0.23$, n=2, two-tailed Student's t-test). For quantification (bottom), the ratio of ATF3/GAPDH protein levels was calculated from the Western Blot data. Data are mean±SEM.
(B) Representative immunohistochemistry images of ipsilateral L4 *Brn3a-Cre^{ERT2};Atf3f/f* DRG neurons 1w after sciatic nerve crush stained for ATF3 (red), NF200 (green) and DAPI (blue). ATF3 expression is strongly induced in vehicle treated (*Atf3* WT) DRG neurons (top) but weakly induced in tamoxifen treated (*Atf3* cKO) DRG neurons (bottom) after sciatic nerve crush.
(C) Recovery of sensory function measured by pinprick assay in vehicle and tamoxifen treated *Brn3a-Cre^{ERT2};Atf3f/f* mice after sciatic nerve crush. Sciatic nerve crush causes a loss of sensory responses in the ipsilateral hindpaw, followed by a recovery over time associated with sensory neuron regeneration. The pinprick responses of vehicle treated *Brn3a-Cre^{ERT2};Atf3f/f* mice (n=8, black line) recover to baseline within 16d after sciatic nerve crush (1-way repeated measures within subjects ANOVA, lower bound $F(1,7) = 343$, $P = 3.3\text{x}10^{-7}$). The pinprick responses of tamoxifen treated *Brn3a-Cre^{ERT2};Atf3f/f* DRG mice (n = 7, red line) show a significant delay in the time course of sensory function recovery (2-way repeated measures between subjects ANOVA, $F(1, 13) = 40.2$, $P = 2.6\text{x}10^{-5}$, Bonferroni post-hoc, *** $P < 0.001$), suggesting a slower rate of sensory neuron regeneration.
(D) Dot plot of neuronal subtype-specific marker genes (rows) in neuronal subtypes (columns) from naive *Atf3f/f* (WT, orange circles) or *Slc17a6-Cre;Atf3f/f* (cKO, purple circles) DRGs. The fraction of nuclei expressing a marker gene is calculated as the number of nuclei in each cell type that express a gene (> 0 counts) divided by the total number of naive nuclei in the respective cell type. Expression in each cell type is calculated as mean expression of marker gene relative to the highest mean expression of that gene across cell types and genotypes.
(E) Bar plot showing percent of nuclei 7d after sciatic crush [100 * crush nuclei / (naive + crush nuclei)] within each neuronal cluster (top row) and violin plots showing injury score (second row, injury score as in Figure 4F) and $\log_2$ expression of selected injury-induced genes in each cluster (third to fourth rows). Note that sciatic crush only injures approximately 50% of lumbar DRG neurons, so there is a greater fraction of crush neurons that co-cluster with naive neurons than is observed in SpNT. Cluster ID (x-axis) corresponds to cluster number assignment from Seurat (see methods). Clusters are classified as injured state (red) if > 90% of nuclei in the cluster are derived from sciatic crush mice (circled clusters in Figure 7B). All other clusters are classified as naive state (green).
(F) UMAP plot of 10,000 randomly sampled neurons that passed quality control from WT and *Atf3* cKO mice. Clusters are colored by the K-nearest neighbors cluster ID assigned by Seurat. The names of each cluster reported in Figure S7E are overlaid on their respective cluster.

(G) Box plot showing the injury score in WT and *Atf3* cKO mice 7d after crush. Scores are normalized to its naive average for each genotype. Boxes indicate quartiles of expression, and whiskers are 1.5-times the interquartile range (Q1-Q3). Median is a black line inside each box. ***$P < 0.001$ two-tailed Student's t-test.
(H) Quantification of Nissl+ DRG neurons in L4 DRG sections from *Slc17a6-Cre;Atf3f/f* cKO (n=4 sections, red) and *Atf3f/f* WT (n=4 sections, black) mice 1w after SpNT. There is no significant difference in DRG neuron density ($P = 0.71$, two-tailed Student's t-test), suggesting an absence of detectable DRG neuronal death at this time point. Data are mean ± SEM.
(I) Bar graph showing the number of early injury-induced transcription factor binding motifs in the 1,030 cell-type-specific genes (see Table S2). As a control, we identified the number of transcription factor binding motifs enriched in 1,030 randomly-selected expressed genes, and repeated this analysis 1000 times. Gray bars show the average number of transcription factor binding motifs enriched in these 1000 sets of 1,030 randomly-selected expressed genes.
(J) Regulation of the 524 common injury-induced genes (rows, from Figure 4C, Table S4) after SpNT, crush, ScNT, and embryonic development. Heatmap shows the $\log_2$FC from differential expression analysis of injured state nuclei in each injury model compared to all naive nuclei as well as the $\log_2$FC between RET+ DRG neurons at 3 embryonic time points (E12.5, E14.5, E18.5) compared to adult RET+ DRG neurons (see methods).
cLTMR = C-fiber low threshold mechanoreceptor; PEP = peptidergic nociceptor; NP = non-peptidergic nociceptor; NF = *Nefh*+ A-fiber low threshold mechanoreceptors; SST = *Sst*+ pruriceptors.